

Petrography and Mineralogy of the Sediments of Ox-Bow Lake from the Ganga Alluvial Plain, India: Implications for Provenance and Tectonic Setting

ABSTRACT

Detailed petrographic, heavy mineral, petrofacies and XRD investigations were conducted on nineteen sediments samples of ox-bow lake from the Ganga plain. The grains are angular to sub-rounded in shape, with some sub-rounded quartz grains. The dominant constituents of the framework grains are primarily quartz, followed by rock fragments, feldspar, mica, and heavy minerals. The majority of the quartz grains are monocrystalline, while the remaining are polycrystalline. Monocrystalline quartz commonly exhibits undulatory extinctions, whereas polycrystalline quartz grains display both distinct and suture intercrystallite boundaries. The feldspar category comprises both fresh and altered varieties, including plagioclase and microcline. Additionally, the presence of biotite, as well as large flakes of muscovite and mica, has been observed. Within the rock fragments, various types such as quartzite, schist, gneiss, phyllite, chert, sandstone, limestone, and siltstone can be found. The heavy minerals encompass a range of minerals such as tourmaline, garnet, opaque, zircon, andalusite, kyanite, sillimanite, staurolite, actinolite/tremolite, hornblende, biotite, rutile, muscovite, chlorite, apatite and zoisite. Petrographic investigations reveal that sediments of ox-bow lake are sublitharenites. Heavy mineral analyses also confirm the possibility of mixed provenance for the ox-bow lake sediments. The ox-bow lake petrofacies indicate their derivation from cratonic interiors, as well as recycled orogenic and quartzose recycled provenances, under semi-humid to humid climatic conditions. The clay mineral abundance endorses the interpretation arrived out from petrofacies plots for the provenance and tectonic setting of ox-bow lake sediments. According to the above discussion on lighter and heavy minerals, the sediments of the ox-bow lake originated from a variety of low-grade to high-grade metamorphic rocks as well as acid and basic igneous rocks.

Key words: Petrography, XRD, Provenance, ox-bow lake, Ganga Plain

1. INTRODUCTION

The petrographic studies of the clastic sediments in conjunction with paleocurrent analyses are effectively used to constrain source lithology and source area as well as geotectonic setting [1]. Sedimentary petrography represents a classical fundamental tool for provenance analysis, widely used to trace detrital sources and reconstruct the geological history of continents, the evolution of drainage systems, and reveal erosional patterns and landscape changes [2,3,4]. A most useful and sensitive complementary approach to determine sediment provenance, applied since the dawn of modern geology, is provided by the analysis of dense minerals [5,6,7]. The sands are primarily composed of mineral grains and rock fragments that have naturally been decomposed in consequence of weathering and erosion of source rocks. Primary minerals may be destroyed or altered by chemical weathering or abrasion / attrition during transportation enroute to the depocenter [8,9,10,11,12,13,14,15,16,17,18,19,20]. Many researchers have attempted to genetically classify detrital quartz since it is an essential and major component of clastic sediments and

is a characteristic parameter for provenance establishment. The detrital quartz grains were initially studied by [21]. [22,23] proposed a genetic classification of detrital quartz into three categories later on. On the basis of extinction, inclusion, and grain shape, igneous quartz (plutonic, volcanic, and vein quartz), metamorphic quartz (recrystallized, schistose, and stretched quartz), and reworked sedimentary quartz are distinguished.[24] changed Kryline's plutonic quartz to common quartz because most quartz from other origins (metamorphic, vein, etc.) have same features. [24] used empirical scheme to classify detrital quartz based on extinction and inclusions.[25] found that undulatory extinction is not a reliable indicator of quartz provenance. [26] identified four types of quartz, one of which being cryptocrystalline quartz (chert). Chert has been described as microcrystalline quartz, cryptocrystalline quartz, and chalcedonic quartz by several researchers [26,24]. Chert is classified into four types: fine-grained, coarse-grained, specular, and silty [27]. The importance of feldspar in terms of source, Paleoclimate, and tectonism has been proposed by number of workers, e.g. [28,29,30,31,32,33,24,34,27,10]. Authigenic feldspar is thought to be a criterion for determining marine origin.[24,27,35] discussed the significance of metamorphic, sedimentary, and volcanic rock fragments. The heavy minerals contained in clastic sediments / sedimentary rocks are also employed as a guide for source-rock characterization, lithological variation, mineral zonation, and dispersal pattern [36,37,7]. Number of assemblages of heavy minerals have been characterized and linked to their probable parent rock [38,39,40,35,26,41,42,24,43]. Since petrographic study of ox-bow lake sediments has not been done so far, this work based on petrological data, aims to analyze the provenance, paleoenvironment and tectonic setting of the Ganga basin.

1.1 DESCRIPTION OF STUDY AREA

The study area of this research work lies between latitude (27°58'- 28°38') and longitude (78°50'- 79°19'). This study is concerned with the sediments of ox-bow lake in parts of upper Ganga Plain for their petrography with the objectives of inferring provenance characteristics and tectonic setting. The sediment samples for this study were collected from various sites located in and around ox-bow lake regions. It was tried to encompass maximum physical variation of sediments both in lateral and vertical dimensions. To account for vertical variations, samples were collected from different horizons of sediment strata from deepest possible points. Thicknesses of the deposits as well as textural and structural variability were the guiding factors for selection of trench sites.

1.2 Geology of Study Area

The Ganga Plain occupies a central position in the Indo-Gangetic Plains, exhibiting many fluvial landforms such as abandoned channels, meander cut-offs, ox-bow lakes, and ponds. The current highly diversified fluvial geomorphology of the Ganga Plain is a result of climate changes, tectonic activity, and base-level changes during the Late Quaternary [44][45]. Most of the lakes and ponds were formed during the Late Pleistocene-Early Holocene due to channel abandonment, influenced by tectonic activity and changing climatic conditions[46][47]. Its expanse stretches from the Aravalli-Delhi ridge in the west to the Rajmahal hills in the east, encompassing the Himalayan foothills (Siwalik Hills) in the north and the Bundelkhand-Vindhyan-Hazaribagh plateau in the south. Positioned between latitudes 24°N and 30°N and longitudes 77°E and 88°E, the Ganga Plain has a length of about 1000 kms and a width of approximately 500 km, with a gradual thinning from west to east. [48] proposed the existence of WNW-ESE and E-W trending weak zones within the

alluvium, influencing the river course and sedimentation patterns. The substantial sediment volumes in Bengal and Indus fans suggest that the foreland basin has been consistently receiving sediments from the Himalaya for at least the past 20 million years [49]. The Ganga basin is identified as a peripheral foreland basin, situated in front of an elevating mountain chain, the Himalaya. This positioning is a consequence of the collision between the Asian and Indian continents, involving the under thrusting of deformed lithosphere [50,51,52,53,54]. Comprising all essential component of a foreland basin system, the Ganga plain basin includes an orogen (the Himalaya), deformed foreland basin deposits adjacent to the orogen (Siwalik hills), a depositional basin (Ganga Plain), and a Peripheral cratonic bulge (Bundelkhand Plateau) [55]. The origination of this foreland basin likely dates back to the early Miocene [56,57]. During the initial phase in the Early Miocene, the foreland basin exhibited relatively small dimensions with minor subsidence [58]. This foreland basin underwent development in the Middle Miocene following significant lithospheric flexure and basin subsidence. From the Middle Miocene to the Middle Pleistocene (covering the deposition of the lower to upper Siwalik Group), the northern segment of the Ganga Plain experienced uplift and thrusting basin ward, causing the Ganga basin to shift southward (toward the craton) in response to thrust loading in the orogen [55]. During this period, [59] characterized the Ganga foreland basin as an "underfilled basin," denoting a topographic low situated between the thrust belt (Himalaya) and the peripheral bulge. However, the underfilled status of the Ganga Plain foreland basin does not result from a lack of sediment supply; rather, it is due to the efficiency of a transport system that redirects the majority of sediment to be deposited in the Ganga delta and Bengal fan. Consequently, the Ganga Plain foreland basin is considered a mature, underfilled basin, marked by an excess of sediment and ongoing sedimentation through fluvial processes. [60] proposed that the Ganga foreland basin has been predominantly influenced by a transverse river system since the Pliocene, attributed to erosional driven uplift and symmetric subsidence of the foreland. In contrast, the Indus basin is characterized by longitudinal river systems due to tectonically driven uplift and asymmetric subsidence of the foreland. During the Plio-Pleistocene period, substantial sediment fluxes, along with reduced asymmetric subsidence and uplift in the proximal foreland, caused the progradation of drainage systems and the displacement of the master stream (Ganga River) to the edge of the current foreland basin. The Ganga River, emerging from the foothills at Devprayag and Haridwar as a trunk river, gains this status through the convergence of several notable tributaries, including the Bhagirathi, Alaknanda, and Mandakini, which flow through various parts of the Himalayas [61]. The total catchment area of the Ganga River is 7,811 km², with 2,328 km² being snow-bound. Upon exiting the hilly tract, the Ganga River flows in a south-eastern direction, traversing the central part of the Gangetic Plain. It serves as the main trunk channel, receiving numerous tributaries on its journey towards the Bay of Bengal. In its youthful stage, the Ganga River begins at the Gangotri Glacier in the Himalayas. During this phase, the river has a steep gradient, flows rapidly, and carves through deep valleys and gorges. It meanders extensively in regions such as Uttar Pradesh and Bihar, where cities like Allahabad (Prayagraj), Varanasi, and Patna are located along its winding paths. In these areas, the river creates wide loops and bends, demonstrating a balance between erosion and deposition. In its late old stage, the Ganga River forms a delta in the Sundarbans region of West Bengal and Bangladesh. In its oldest stage, a stream significantly slows down and can only transport smaller sediments such as silt. This stage features meanders that curve even more than those in the mature stage. Due to the larger size of these meanders, ox-bow lakes are often formed. An ox-bow lake is a horseshoe-shaped lake found on the floodplain of a stream. Meanders may create

a loop with only a narrow neck of land separating their outer banks. During a heavy flood, the stream may cut through this neck, leaving the loop as a cut-off. This cut-off section then becomes an ox-bow lake.

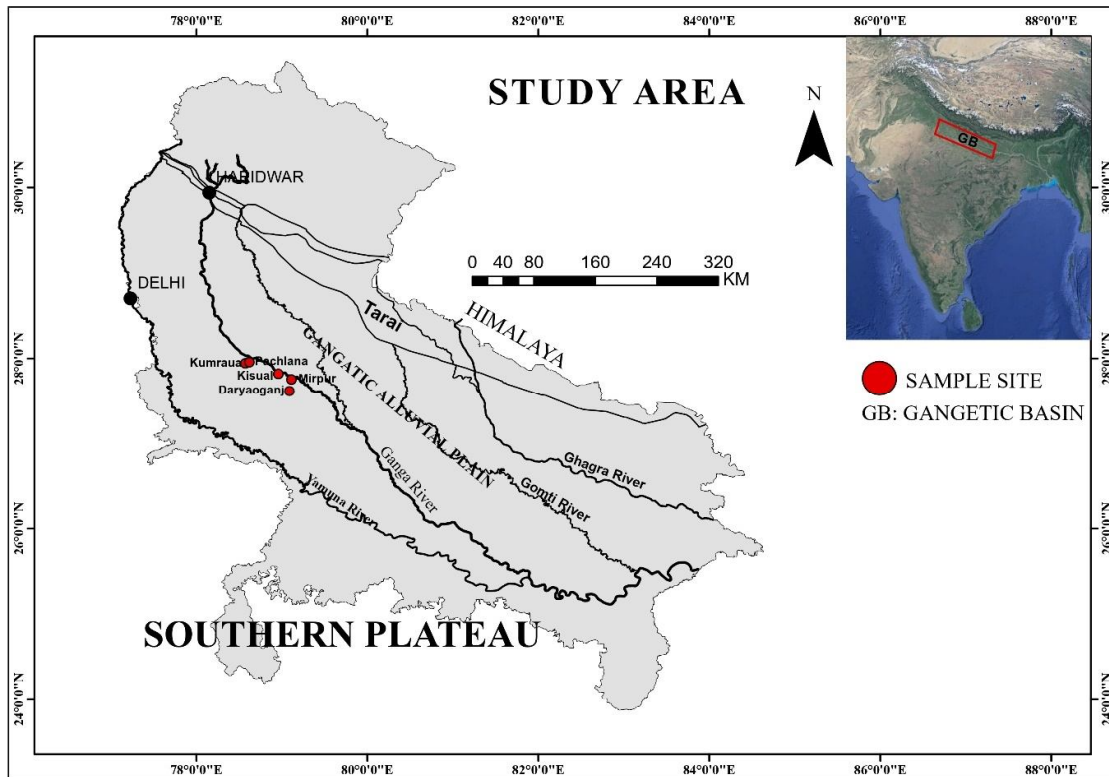


Fig.1. Simplified map of Gangetic plain (modified from Singh, 1996) showing sampling sites ox-bow lakes.

2. MATERIAL AND METHODS

The present study assesses the detrital mineral composition of ox-bow lake sediments, specifically focusing on the quantitative and qualitative evaluation of sand through the examination of 28 thin sections within the study area. Samples were collected from various locations, including 3 from Kumraua, 4 from Pachlana, 9 from Daryaoganj and 3 from Kisaul. These selections were made to ascertain the modal composition and other petrographic characteristics of the sand samples. For quantitative analysis, a consistent count of approximately 200-300 grains per slide was conducted to ensure uniform coverage of thin sections. Identification of K-feldspar grains was achieved by staining with a cobaltinitrite solution. The terminology employed for describing different types of quartz and other framework elements follows [62,24]. All grain parameter data were compiled and recalculated to 100% for various compositional diagrams, using a specific ternary diagram for sandstone classification, Petro facies analysis, and interpretation of the paleotectonic setting of the provenance. This methodology follows the approaches outlined by [8,2,27]. To understand the paleoclimatic conditions of the provenance, grain parameter ratios and groupings were determined using several bivariant log/log plots, as described by [17]. According to [63], the relative abundance of heavy mineral species is size-dependent. It is postulated that the size fraction finer than the modal category records the highest concentration of heavy minerals

[64]. Consequently, in this study, sediments classified finer than the modal class were selected for heavy mineral analysis, employing [65] approach for heavy mineral separation. For the heavy mineral analysis of sediments samples were subjected to processing. Bromoform was used as the heavy liquid to separate the dense minerals from the sand fraction in a separating funnel. The separated samples were then collected for petrographic analysis in thin sections.

Table 1. Grain Parameters used in the modal analysis after [8,2,27,66]

| | | |
|---|---------------------------|--|
| A | Quartzose Grains | $Qt=(Qm+Qp)$ |
| | | Qt= Total quartz grain |
| | | Qm=Mono-crystalline quartz grain |
| | | Qp=Poly-crystalline quartz grain |
| B | Feldspar Grains | $F=(P+K)$ |
| | | F=Total feldspar grain |
| | | P=Plagioclase feldspar grain |
| | | K=Potash Feldspar |
| C | Unstable Lithic fragments | $L=(Lv+Ls)$ |
| | | L=Total unstable lithic fragments |
| | | Lv=Volcanic/metavolcanic lithic-fragments |
| B | Total Lithic Fragments | Ls= Sedimentary/metasedimentary lithic fragments |
| | | $Lt=(L+Qp)$ |
| | | Lc=Extra basinal detrital limeclasts (not included in L or Lt) |

3.RESULTSAND DISCUSSION

3.1 Detrital mineral composition

The studied sand samples are primarily comprised quartz, followed by sedimentary and metamorphic rock fragments, feldspar, micas, and heavy minerals. The average composition of detrital minerals in the ox-bow lake are monocrystalline quartz (82.64%), polycrystalline quartz (3.59%), rock fragment (9.70%), feldspar (1.90%) mica (1.69) and heavy minerals (0.48%) showed in following (Table 1).

3.1.1 Quartz(Q)

Quartz is the predominant constituent, and its variations have been classified according to [24] scheme. The majority of quartz grains are monocrystalline, accompanied by some polycrystalline grains. In the ox-bow lake, the quartz content ranges from (Qm, 71.81%-89.46%, with an avg. of 82.64%, and Qp, 0.28%-6.56%, avg. 3.59%). Monocrystalline quartz typically exhibits undulatory extinction. Polycrystalline quartz grains display both sharp and sutured intracrystalline boundaries in all sediment samples from the lakes.

3.1.2 Feldspar(F)

The detrital feldspar, occurring in small amounts, comprises both fresh and altered varieties. In the ox-bow lake sediments, two varieties of feldspar have been identified based on their abundance: K-Feldspar (microcline-orthoclase) and plagioclase (Table.2). Their ranges in the ox-bow lake are (Plagioclase, 0%-2.25%, avg. 0.58%, and K-Feldspar, 0.02%-3.08%, avg. 1.32%). Most plagioclase grains are colorless and appear grey in cross-nicols. They exhibit a prismatic outline, appearing angular to subrounded. Different twinning laws are evident in the plagioclase. Microclines manifest as prismatic and rounded broken grains, representing cross-hatch twinning. Altered feldspars (plagioclase and microcline) exhibit a dusty appearance under plain-polarized light, and their interference colors range in shades of grey and brown.

3.1.3 Rock Fragments (Lt)

Sedimentary and metamorphic rock fragments exhibit sparse distribution in ox-bow lake sediments. The concentration of rock fragments in ox-bow lake sediments ranges from (4.68%-14.91%, avg. 9.07%). Quartzite and schist emerge as the most prevalent types of rock fragments in the studied sands, with some recorded fragments of gneiss and phyllite. Sedimentary rock fragments encompass chert, sandstone, limestone, and siltstone, displaying a subrounded to well-rounded shape, comparable in size to surrounding quartz grains. Rock fragments are present in varying proportions within the sediments of the ox-bow lake.

3.1.4 Accessory Minerals

In addition to the principal mineral components several accessory minerals such as Mica (Biotite, Muscovite) grains are present in minimal amounts in all the sediment samples of the ox-bowlake. In ox-bow lakesediments sample their percentage ranges from (1.01%-2.50%, with an avg. of 1.69%). Both muscovite and biotite manifest as tiny to large elongate flakes with frayed ends. These flakes occasionally exhibit mechanical deformation, likely caused by pressure from accompanying quartz grains. Biotite grains typically display a yellowish-brown color. These minerals are derived primarily from metamorphic rocks, with occasional contributions from plutonic and, rarely, volcanic rocks. Muscovite exhibits greater chemical stability compared to biotite. Generally, the abundance of micas in sediments suggests a metamorphic provenance. The presence of micas in the ox-bow lake sediments indicates their likely derivation from sources such as granites, pegmatites, or schist.

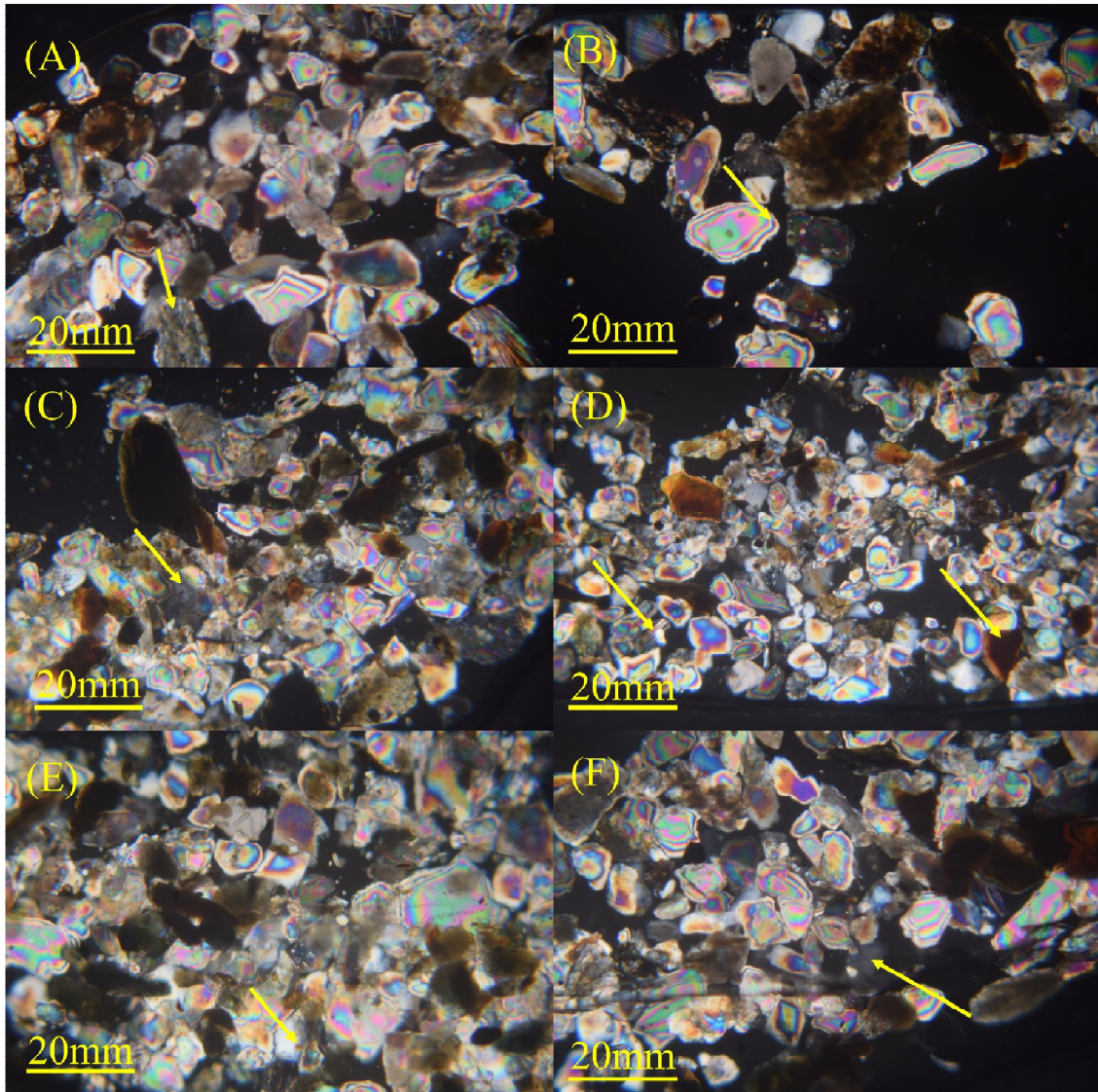


Fig.2. Photos of selected petrographic slides of ox-bow lake sediments showing. (A) Rock fragments, (B) Common quartz, (C) Metamorphic quartz, (D) Microcline grain, and Biotite (E&F) stretched metamorphic quartz.

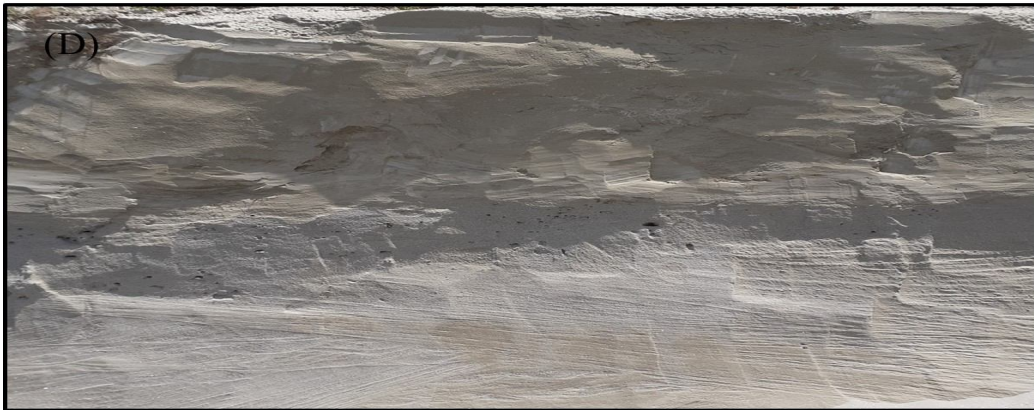


Fig.3. Field photographs from the ox-bow lake of Gangaplain with significant importance, such as: (A&B) Planar stratification; (C&D) showing large scale planar cross stratification.

Table 2.Percentage of mineralogical composition of the ox-bow lake sediments. Legends: Qm-Monocrystalline Quartz, Qp-Polycrystalline Quartz, RF-Rock Fragment, K-Feldspar (Orthoclase and or Microcline), KM-Kumraua, PH-Pachlana, DG-Daryaoganj, KS-Kisaul.

| S.No. | Sample No. | Qm | Qp | Mica | RF | Feldspar | | Heavy Minerals |
|----------------|------------|--------------|-------------|-------------|-------------|--------------|-------------|----------------|
| | | | | | | Plagioclase. | K-Felds. | |
| 1 | KM1 | 80.47 | 3.46 | 1.24 | 12.03 | 0.50 | 1.95 | 0.35 |
| 2 | KM2 | 80.50 | 6.32 | 1.09 | 10.09 | 0.40 | 1.00 | 0.61 |
| 3 | KM3 | 83.53 | 1.98 | 1.57 | 12.71 | - | 0.02 | 0.19 |
| 4 | PH1 | 85.30 | 2.39 | 2.18 | 8.88 | - | 0.63 | 0.62 |
| 5 | PH2 | 86.05 | 5.68 | 2.50 | 4.68 | - | 0.87 | 0.22 |
| 6 | PH3 | 84.61 | 6.19 | 2.11 | 5.40 | - | 0.86 | 0.82 |
| 7 | PH4 | 85.39 | 3.34 | 2.14 | 5.80 | 0.58 | 1.82 | 0.93 |
| 8 | DG1 | 83.33 | 1.22 | 2.04 | 9.48 | 1.21 | 2.28 | 0.44 |
| 9 | DG2 | 84.03 | 2.46 | 2.34 | 9.21 | 0.36 | 1.00 | 0.60 |
| 10 | DG3 | 89.46 | 1.45 | 1.29 | 6.18 | - | 1.23 | 0.38 |
| 11 | DG4 | 84.83 | 3.44 | 1.82 | 8.89 | - | 0.77 | 0.27 |
| 12 | DG5 | 85.69 | 0.28 | 1.01 | 12.08 | - | 0.35 | 0.60 |
| 13 | DG6 | 82.95 | 1.98 | 1.24 | 10.24 | 0.94 | 2.12 | 0.52 |
| 14 | DG7 | 77.50 | 3.56 | 1.03 | 16.19 | - | 1.09 | 0.63 |
| 15 | DG8 | 79.20 | 4.67 | 1.61 | 9.80 | 2.25 | 2.29 | 0.18 |
| 16 | DG9 | 79.23 | 5.38 | 1.20 | 11.87 | 0.58 | 1.09 | 0.66 |
| 17 | KS1 | 85.33 | 3.22 | 2.09 | 8.80 | - | 0.19 | 0.38 |
| 18 | KS2 | 81.00 | 4.68 | 2.41 | 7.01 | 2.10 | 2.40 | 0.39 |
| 19 | KS3 | 71.81 | 6.54 | 1.22 | 14.91 | 2.12 | 3.08 | 0.32 |
| Average | | 82.64 | 3.59 | 1.69 | 9.70 | 0.58 | 1.32 | 0.48 |

3.1.5 Heavy Minerals

The heavy minerals that have been separated are calculated as a percentage of each sample. Each thin section contained between 22 and 80 detrital heavy mineral grains, which were counted manually under the microscope to determine the percentage of individual heavy minerals. The heavy mineral species in ox-bow lake sediments are Tourmaline, Garnet, Chlorite, Opaque, Zircon, Kyanite, Sillimanite, Tremolite Actinolite, Staurolite, Hornblende, Biotite, Zoisite, Andalusite, Topaz, corundum and Rutile are among the heavy mineral suites found in the ox-bow lake sediments. The diagnostic properties of the heavy mineral assemblages are summarized below.

Tourmaline: Tourmaline is the most abundant heavy mineral in the sediments sample. The tourmaline abundance in various ox-bow lake sediments is as 30.56% (Mirpur), 30.54% (Kumraua), and 26.15% (Pachlana), 29.34% (Daryaoganj). Tourmaline variants in brown, green, and greenish brown colors are widespread in studied sands. The majority of the

grains are prismatic, although there are some subrounded to well-rounded grains (Plate-III). Tourmaline is highly pleochroic, with striations and show parallel extinction.

Garnet: Garnet is also present in ox-bowlake sediments. The Garnet abundance in ox-bow lake sediments is as 6.81% (Mirpur), 8.02% (Kumraua), 9.73% (Pachlana), 7.32% (Daryaoganj). Dark brown colour garnet variety is widespread instudied sands. Most grains are roughly equidimensional marked with the fractures on the surface (Plate II- j). Grains are mostly angular to subrounded.

Chlorite: Chlorite is heavy mineral occur in minor amount in the ox-bow lake sediments. The abundance of chlorite in ox-bow lake is as 1.20% (Mirpur), 1.14% (Kumraua), and 1.39% (Pachlana), 1.42% (Daryaoganj). It appears as flake that are flat, rounded, or irregular. The grains range in colour from pale green to dark green, with black spots and blue polarization (Plate II-g-h).

Opaque: The opaque is abundant heavy mineral of sediments. The abundance of chlorite in ox-bow lake is as 31.67% (Mirpur), 30.22% (Kumraua), 33.11% (Pachlana) and 31.91% (Daryaoganj). The opaque black grains are angular to subrounded (Plate IV- n).

Zircon: Zircon is also present in ox-bow lake sediments. The abundance of zircon in ox-bow lake 2.37% (Mirpur), 1.49% (Kumraua), 2.18% (Pachlana), 1.79% (Daryaoganj). Zircon grains have angular to subrounded boundaries and are pyramidal in form. Colorless, pink, and pale-yellow zircon is the most prevalent in the ox-bow lake sediments. Inclusions of opaque minerals are present (Plate V-x-y).

Kyanite: Kyanite is found sediments sample. The abundance of kyanite in ox-bow lake is as 2.72% (Mirpur), 5.11% (Kumraua), 2.46% (Pachlana) and 4.76% (Daryaoganj). Only the colorless type of kyanite was found in the examined sediments. The grains range from angular to subrounded and elongated, having rectangular outlines (Platell-I).

Sillimanite: Sillimanite is heavy mineral present in sediment deposits. The abundance of sillimanite in ox-bow lake is as 1.46% (Mirpur), 1.22% (Kumraua), 1.10% (Pachlana) and 1.95% (Daryaoganj). The dominant variety is colorless, followed by a green variety. The grains appear as thin prisms or fibrous having fractured or uneven terminations. The grains are generally subangular to subrounded (Plate IV- o-p).

Staurolite: Staurolite is less abundant heavy mineral of sediments ox-bow lake. The abundance of staurolite in the ox-bowlake is as 1.38% (Mirpur), 1.85% (Kumraua), 3.40% (Pachlana) and 2.93% (Daryaoganj). One variety have been identified straw yellow (dominant) and brownish yellow. The grains are irregular, subangular to subrounded in shape (PlateIV-q).

Actinolite/tremolite: Actinolite/tromolite are found in minor amounts of sediment deposits. The abundance of actinolite/Tremolite in the ox-bow lake is as 1.14% (Mirpur), 2.89% (Kumraua), and 2.30% (Pachlana) and 1.32% (Daryaoganj). Tremolite is dark-brown whereas actinolite is colorless in the ox-bow lake sediments. The grains are often irregular prismatic. The granules of actinolite/tremolite are fibrous in form (Plate V-w-z).

Hornblende: Hornblende is present inthe ox-bow lake sediments. The abundance of hornblende in the ox-bow lake is as 4.07% (Mirpur), 2.45% (Kumraua), and 3.30%

(Pachlana) and 2.89% (Daryaoganj). Hornblende shows a characteristic green color. Usually, the grains are elongate and irregularly terminated (Plate II-k).

Biotite: Biotite is an abundant heavy mineral of ox-bow lake deposits. The abundance of biotite in the ox-bow lake is as 5.32% (Mirpur), 5.40% (Kumraua), 1.84% (Pachlana) and 4.63% (Daryaoganj). Biotite grains are prismatic or flakes with irregular outlines. Pale brown color variety of biotite is common (Plate I-c).

Apatite: Apatite is less abundant heavy mineral of ox-bow lake sediments. The abundance of apatite in the ox-bow lake sediments is as 1.80% (Mirpur), 1.43% (Kumraua), 2.49% (Pachlana) and 2.05% (Daryaoganj). Colorless apatite grains are hexagonal and slightly worn elongated prismatic crystal (Plate I-d-e-f).

Zoisite: Zoisite is also observed in the lake sediments. The modal percentage of zoisite is as 2.40% (Mirpur), 2.42% (Kumraua), 2.92% (Pachlana) and 1.13% (Daryaoganj) in the ox-bow lake sediments. Colorless variety is common (Plate IV-m).

Andalusite: Andalusite is present in sediments of the study area. The percentage varies in ox-bow lake sediments is as 2.50% (Mirpur), 2.26% (Kumraua), and 1.15% (Pachlana) and 1.86% (Daryaoganj). Green and dark green variety are common. Andalusite is angular occasionally prismatic, subrounded and rarely well rounded (Plate I-a-b).

Corundum: Corundum is also present in the sediments. The percentage varies in the ox-bow lake sediments is as 1.14% (Mirpur), 1.49% (Kumraua), and 2.30% (Pachlana) and 2.18% (Daryaoganj). Colorless variety is common. Inhomogeneous color distribution is characteristic. Grains are generally irregular, angular, subrounded and occasionally well rounded (Plate II-l).

Topaz: The Topaz abundance in the ox-bow lake sediments is as 1.46% (Mirpur), 1.01% (Kumraua), 1.84% (Pachlana) and 1.38% (Daryaoganj). Most detrital grains are colorless with a noticeable bluish-white tinge, but pale-coloured yellow, pink, red and blue grains are also reported (Plate IV-r).

Rutile: Rutile is abundant heavy mineral in the sediments of ox-bow lake deposits. Its abundance in the ox-bow lake sediments is as 3.92% (Mirpur), 2.97% (Kumraua), 3.22% (Pachlana) and 4.61% (Daryaoganj). They occur in minor amount brownish red to yellow varieties are commonly present. Grains are generally angular to subrounded. Elongated prismatic forms also occur with rounded pyramidal ends. Rutile grains show high relief, central part is characterized by blood red color and border is dark (Plate III-v1).

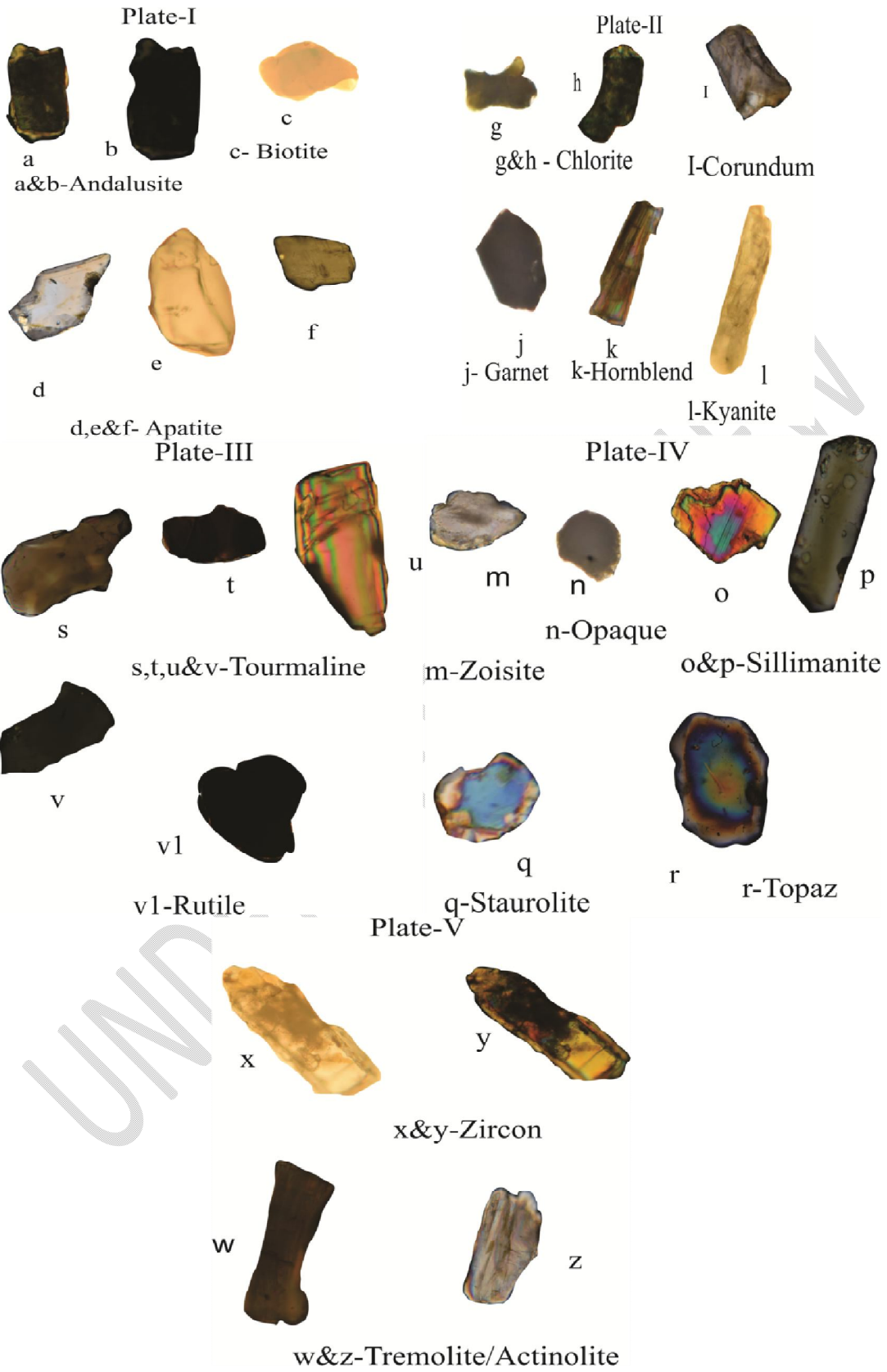


Fig. 4. Heavy mineral assemblage in ox-bow lake sediments of Ganga alluvial plain (Plate I-V).

Heavy minerals play a crucial role in determining provenance [67,68,69,70,71,72,73]. Their shapes and roundness serve as sensitive indicators of abrasion intensity, reflecting the nature of the transport route, distance, agency, and its intensity. Additionally, specific suites or assemblages of heavy minerals align with source rocks and their habitats [35,63,74]. The presence of various heavy mineral species in the ox-bow lake sediments of the Indo-Gangetic Plain suggests that these sediments originated from a diverse array of source rocks. Tourmaline emerges as the dominant heavy mineral, exhibiting various colors. Brown and blue tourmaline varieties likely originated in pegmatites, while the green variety has roots in granitic rocks [3]. Moreover, rounded tourmaline seems to have been derived from a pre-existing sedimentary source, indicating multiple transportation cycles. The presence of kyanite-sillimanite in these sediments suggests the weathering contribution of kyanite-sillimanite-bearing high-grade metamorphic rocks in the source terrain. Colorless garnet may have originated from schists, light pink garnet from acid igneous rocks like granite, and brownish garnet from igneous metamorphic rocks such as crystalline gneisses and schists. Zircon likely came from crystalline igneous and metaigneous rocks, and apatite from acid igneous rocks and pegmatites [75]. Andalusite forms in meta-argillaceous rocks in the contact aureoles around igneous intrusions. Topaz primarily forms in granite pegmatite and gneisses. Corundum is found in various rock types, particularly in Al-rich, Si-poor rocks, such as syenites, quartz-free pegmatites, mica, or chlorite schists.

3.2 Classification of the sediments

To classify the sediments under study using [24] method, all major components were recalculated to 100 percent, and are plotted in Q-F-L ternary diagram (Fig.5). The average composition of framework grains of the ox-bow lake is as follows. Quartz-88.16%, Feldspar-1.94% and Rock fragments-9.90% table (3). All the sediments samples of ox-bow lake plotted near the Q pole, in the sublitharenites field (Fig.5).

Table 3. Percentage of framework modes of the ox-bow lake sediments. Legends: Q=Quartz, F= Feldspar, L= Lithic fragments. KM-Kumraua, PH-Pachlana, DG-Daryaoganj, KS-Kisaul.

| Sample No. | Q | F | L |
|------------|-------|------|-------|
| KM1 | 85.29 | 2.49 | 12.23 |
| KM2 | 88.32 | 1.42 | 10.26 |
| KM3 | 87.04 | 0.02 | 12.94 |
| PH1 | 90.22 | 0.64 | 9.14 |
| PH2 | 94.29 | 0.90 | 4.81 |
| PH3 | 93.55 | 0.89 | 5.57 |

| | | | |
|----------------|--------------|-------------|-------------|
| PH4 | 91.54 | 2.47 | 5.99 |
| DG1 | 86.70 | 3.58 | 9.72 |
| DG2 | 89.11 | 1.40 | 9.49 |
| DG3 | 92.46 | 1.25 | 6.28 |
| DG4 | 90.15 | 0.78 | 9.07 |
| DG5 | 87.38 | 0.35 | 12.27 |
| DG6 | 86.46 | 3.12 | 10.43 |
| DG7 | 82.43 | 1.11 | 16.47 |
| DG8 | 85.40 | 4.62 | 9.98 |
| DG9 | 86.21 | 1.70 | 12.09 |
| KS1 | 90.79 | 0.19 | 9.02 |
| KS2 | 88.16 | 4.63 | 7.21 |
| KS3 | 79.57 | 5.28 | 15.14 |
| Average | 88.16 | 1.94 | 9.90 |

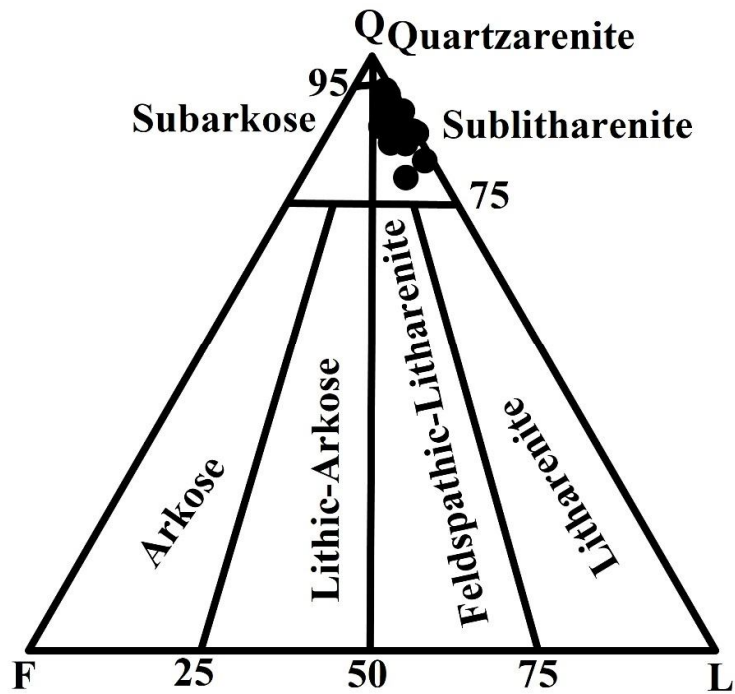


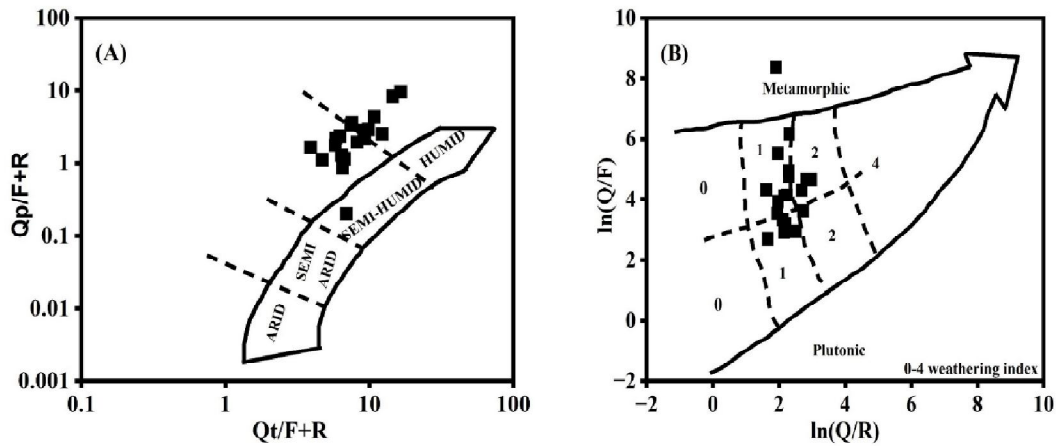
Fig.5.Folk's Q-F-L diagram for sediments of ox-bow lake of Ganga alluvial plain classifying them as sub-lith arenite. Legends: Q- (all forms of quartz, including common quartz, recrystallized metamorphic quartz, stretched metamorphic quartz, and reworked sedimentary quartz), F-All feldspars (Plagioclase, orthoclase, Microcline) L- All forms of fragments (rock including chert).

Table 4. Recalculated detrital modes of the ox-bow lake sediments based on [10]. Legends: KM-Kumraua, PH-Pachlana, DG-Daryaoganj, KS-Kisaul.

| S.No | Sample. No | Qt | F | L | Qm | F | Lt | Qp | Lv | Ls | Qm | P | K | Q/R | Q/F | Qp/F+L | Qt/F+L |
|----------------|------------|--------------|-------------|------------|--------------|-------------|--------------|-------------|----------|-------------|--------------|------------|-------------|--------------|---------------|-------------|-------------|
| 1 | KM-S1 | 85.29 | 2.49 | 12.23 | 81.77 | 2.49 | 15.74 | 25.95 | 0 | 74.05 | 97.05 | 0.6 | 2.35 | 6.98 | 34.31 | 1.76 | 5.80 |
| 2 | KM-S2 | 88.32 | 1.42 | 10.26 | 81.89 | 1.42 | 16.69 | 42.51 | 0 | 57.49 | 98.29 | 0.49 | 1.22 | 8.61 | 62.16 | 3.64 | 7.56 |
| 3 | KM-S3 | 87.04 | 0.02 | 12.94 | 85.02 | 0.02 | 14.96 | 14.92 | 0 | 85.08 | 99.98 | 0 | 0.02 | 6.73 | 4338.50 | 1.15 | 6.72 |
| 4 | PH-S1 | 90.22 | 0.64 | 9.14 | 87.76 | 0.64 | 11.6 | 21.2 | 0 | 78.8 | 99.27 | 0 | 0.73 | 9.87 | 140.08 | 2.17 | 9.22 |
| 5 | PH-S2 | 94.29 | 0.9 | 4.81 | 88.45 | 0.9 | 10.65 | 54.82 | 0 | 45.18 | 99 | 0 | 1 | 19.60 | 105.27 | 9.61 | 16.52 |
| 6 | PH-S3 | 93.55 | 0.89 | 5.57 | 87.17 | 0.89 | 11.94 | 53.39 | 0 | 46.61 | 98.99 | 0 | 1.01 | 16.80 | 105.41 | 8.27 | 14.49 |
| 7 | PH-S4 | 91.54 | 2.47 | 5.99 | 88.09 | 2.47 | 9.43 | 36.53 | 0 | 63.47 | 97.27 | 0.66 | 2.07 | 15.29 | 37.01 | 4.32 | 10.82 |
| 8 | DG-S1 | 86.7 | 3.58 | 9.72 | 85.45 | 3.58 | 10.97 | 11.4 | 0 | 88.6 | 95.98 | 1.39 | 2.62 | 8.92 | 24.24 | 0.86 | 6.52 |
| 9 | DG-S2 | 89.11 | 1.4 | 9.49 | 86.58 | 1.4 | 12.02 | 21.08 | 0 | 78.92 | 98.41 | 0.42 | 1.17 | 9.39 | 63.72 | 1.94 | 8.19 |
| 10 | DG-S3 | 92.46 | 1.25 | 6.28 | 90.99 | 1.25 | 7.76 | 19.01 | 0 | 80.99 | 98.64 | 0 | 1.36 | 14.71 | 73.69 | 2.52 | 12.26 |
| 11 | DG-S4 | 90.15 | 0.78 | 9.07 | 86.63 | 0.78 | 12.59 | 27.91 | 0 | 72.09 | 99.11 | 0 | 0.89 | 9.93 | 115.60 | 2.83 | 9.15 |
| 12 | DG-S5 | 87.38 | 0.35 | 12.27 | 87.09 | 0.35 | 12.56 | 2.53 | 0 | 97.47 | 99.6 | 0 | 0.4 | 7.12 | 249.85 | 0.20 | 6.92 |
| 13 | DG-S6 | 86.46 | 3.12 | 10.43 | 84.44 | 3.12 | 12.44 | 17.37 | 0 | 82.63 | 96.44 | 1.09 | 2.47 | 8.29 | 27.74 | 1.28 | 6.38 |
| 14 | DG-S7 | 82.43 | 1.11 | 16.47 | 78.81 | 1.11 | 20.09 | 19.66 | 0 | 80.34 | 98.61 | 0 | 1.39 | 5.01 | 74.45 | 1.12 | 4.69 |
| 15 | DG-S8 | 85.4 | 4.62 | 9.98 | 80.65 | 4.62 | 14.73 | 32.28 | 0 | 67.72 | 94.58 | 2.69 | 2.73 | 8.56 | 18.49 | 2.21 | 5.85 |
| 16 | DG-S9 | 86.21 | 1.7 | 12.09 | 80.73 | 1.7 | 17.57 | 32.67 | 0 | 67.33 | 97.94 | 0.72 | 1.35 | 7.13 | 50.67 | 2.37 | 6.25 |
| 17 | KS-S1 | 90.79 | 0.19 | 9.02 | 87.48 | 0.19 | 12.33 | 26.78 | 0 | 73.22 | 99.78 | 0 | 0.22 | 10.06 | 477.73 | 2.91 | 9.85 |
| 18 | KS-S2 | 88.16 | 4.63 | 7.21 | 83.34 | 4.63 | 12.03 | 40.03 | 0 | 59.97 | 94.74 | 2.46 | 2.81 | 12.22 | 19.04 | 3.38 | 7.44 |
| 19 | KS-S3 | 79.57 | 5.28 | 15.14 | 72.93 | 5.28 | 21.79 | 33.76 | 0 | 66.24 | 93.25 | 2.75 | 4 | 5.25 | 15.06 | 1.65 | 3.90 |
| Average | | 88.16 | 1.94 | 9.9 | 84.49 | 1.94 | 13.57 | 28.1 | 0 | 71.9 | 97.73 | 0.7 | 1.57 | 10.02 | 317.53 | 2.85 | 8.34 |

3.4 Paleoclimate

Detrital methodology has also been used to depict the paleoclimate that prevailed at the time of deposition. Sedimentary processes, along with paleoclimate, tectonics, and modes of transportation, significantly affect the composition of the sandstone and its depositional basin [17]. Along with [17,76] also provided confirming opinions on the paleoclimatic history. Therefore, the detrital were recalculated in terms of $Q_p/(F+L)$ and $Q_t/(F+L)$ and studied by plotting on the bivariate log/log graph [17], which is the most prominent way to investigate paleoclimatic conditions. The area on this graph is primarily used to depict the prevailing climatic conditions at the time of sediments deposition. The $Q_p/(F+L)$ ratio of the ox-bow lake sediments ranges from 0.20% to 9.61% (average 2.85%), while the $Q_t/(F+L)$ ratio of the sediments ranges from 3.90% to 16.52% (average 8.34%). This plot clearly shows that the sediments of ox-bow lake was derived from the provenance area under semi humid to humid climatic conditions (Fig.6A). In order to ascertain the relief and the paleoclimate of the source region, [76] provided certain semi-quantitative weathering indices. The sediments of ox-bow lake have low to moderate weathering indices ranging from 1 to 2, as shown in the bivariate plot of $\text{Log } Q/F$ and $\text{Log } Q/L$ (Fig.6B). These indices indicate that the sediments are mainly derived from moderate terrain (hilly) platforms under a temperate sub-humid to tropical humid climate.



| Semi-quantitative Weathering Index | Physiography (relief) | | |
|------------------------------------|-----------------------|---------------------|----------------|
| | High (mountains) | Moderate (hills) | Low (plain) |
| Semi-Arid and mediterranean (0) | 0 | 0 | 0 |
| Temperate subhumid (1) | 0 | 1 | 2 |
| Tropical humid (2) | 0 | 2 | 4 |

Fig.6. (A) Bivariant log/log plot of $Qp/(F+R)$ against $Qt/(F+R)$ after [17]. (B) Bivariant log-ratio plot of Q/F against Q/R after [76]. Field 1-4 refers to the semi-quantitative weathering indices defined on the basis of relief and climate.

3.4 Petro facies and tectono-provenance

For this present study, four triangular diagrams proposed by [10] have been utilized, namely Qt-F-L, Qm-F-Lt, Qp-Lv-Ls, and Qm-P-K (Fig.7,8,9 &10). Both the Qt-F-L plots and the Qm-F-Lt plots represent full grain populations but with different concentrations. The Qt-F-L diagram highlights provenance, relief, weathering, and transport mechanisms, as well as source rock characteristics based on total quartzose, feldspathic, and lithic components. In this diagram, the data from ox-bow lake sediments are mostly plotted in the recycled orogen provenance field (Fig.7), indicating that they are derived from metasedimentary and sedimentary rocks deposited along former passive continental margins [8,10]. A few samples fall into the continental block provenance, indicating contributions from the craton interior with basement uplift. To emphasize the source rocks, all unstable-lithic fragments, including polycrystalline quartz, are represented as Lt in the Qm-F-Lt diagram. The sediments sample data are plotted in both the recycled orogen and craton interior in this diagram (Fig.8). Because the amount of polycrystalline quartz tends to decrease due to recycling and weathering, the ratio of monocrystalline quartz to polycrystalline quartz represents the history of sediments and sedimentary rocks [16]. The Qp-Lv-Ls triangular plot, based on the rock fragment population, displays the polymineralic component of the source region and provides a more refined image of the tectonic elements. The Qp-Lv-Ls triangular plot emphasizes the type of the orogenic environment from which the detritus was derived [10]. According to [77,78], the Qp-Lv-Ls triangular plot is a useful tool for distinguishing detrital modes of suture belts from magmatic arcs and rifted continental margins. The studied data fall into a collision suture and fold thrust belt setting (Fig.9), reflecting little or no contribution from the volcanic source. The Qm-P-K plot demonstrates that ox-bow lake sediments received contributions from the continental block basement uplift provenance (Fig.10) and is reflected in mineralogical maturity of the sediments and stability of the source area.

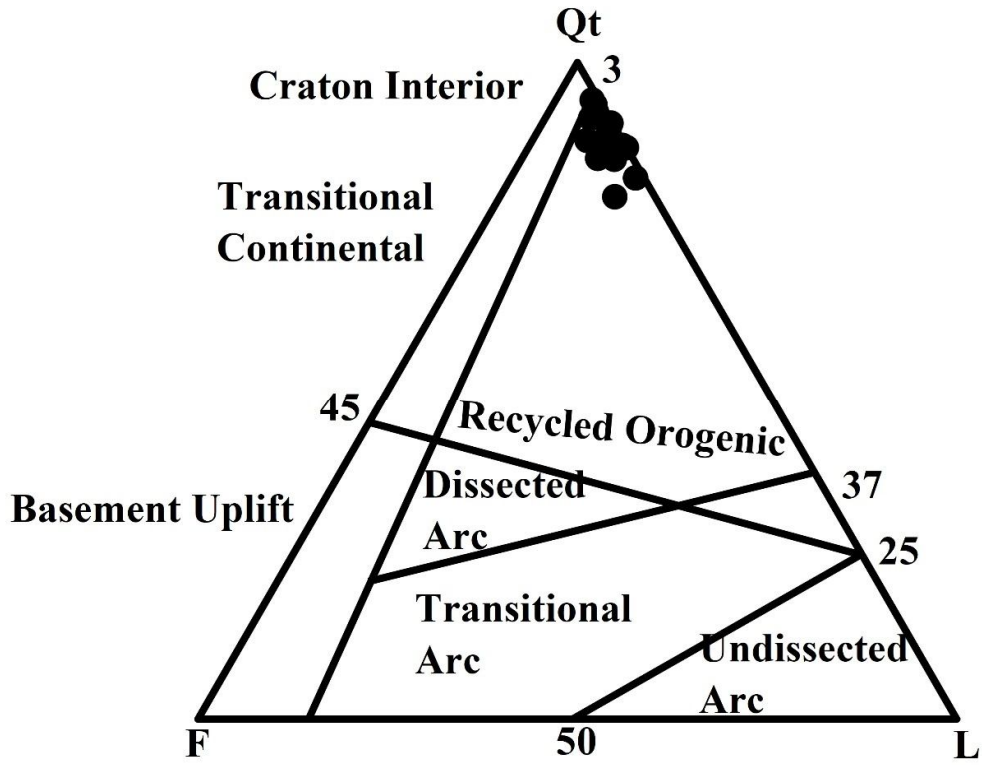


Fig.7.Qt-F-L plot for ox-bow lake sediments of Ganga alluvial plain.

UNDER P&T

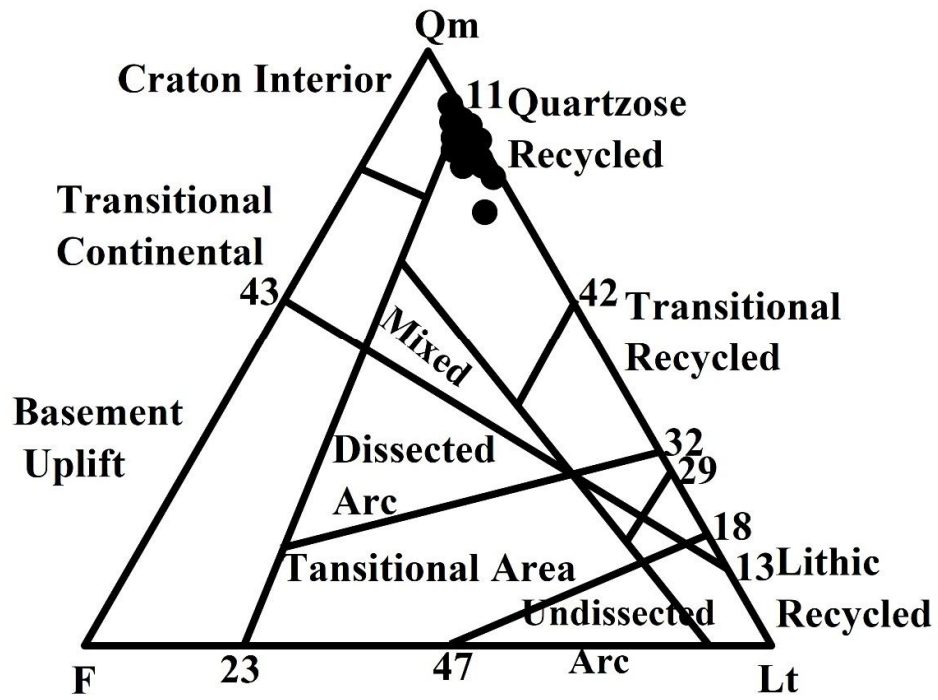


Fig.8. Qm-F-Lt plot for ox-bow lake sediments of Ganga alluvial plain.

UNDER PEE

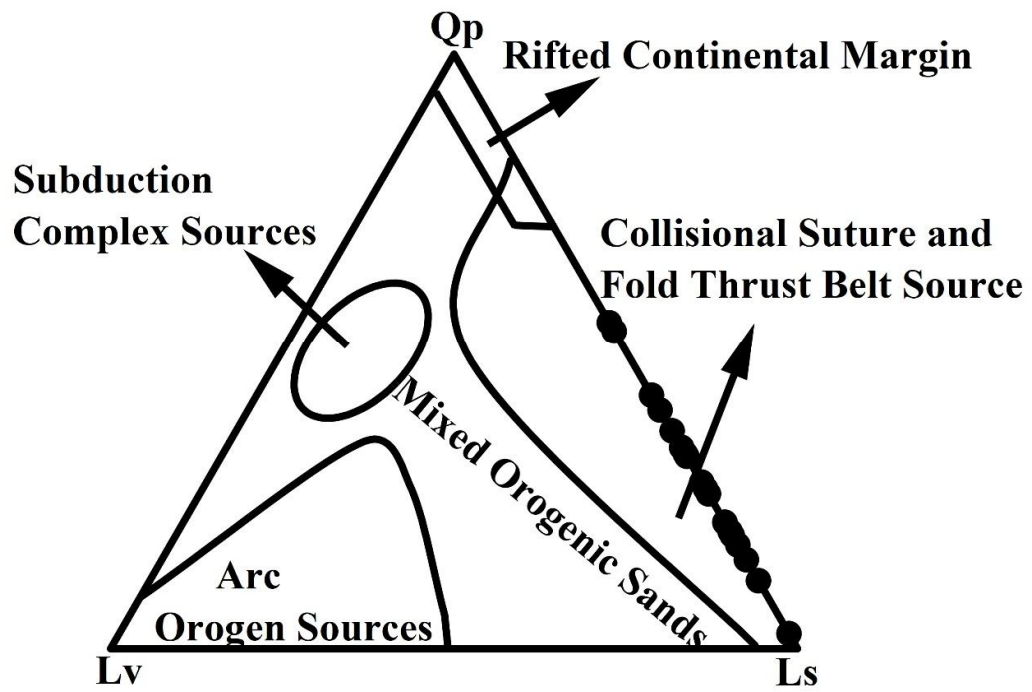


Fig.9.Qp-Lv-Ls plot for ox-bow lake sediments of Ganga alluvial plain.

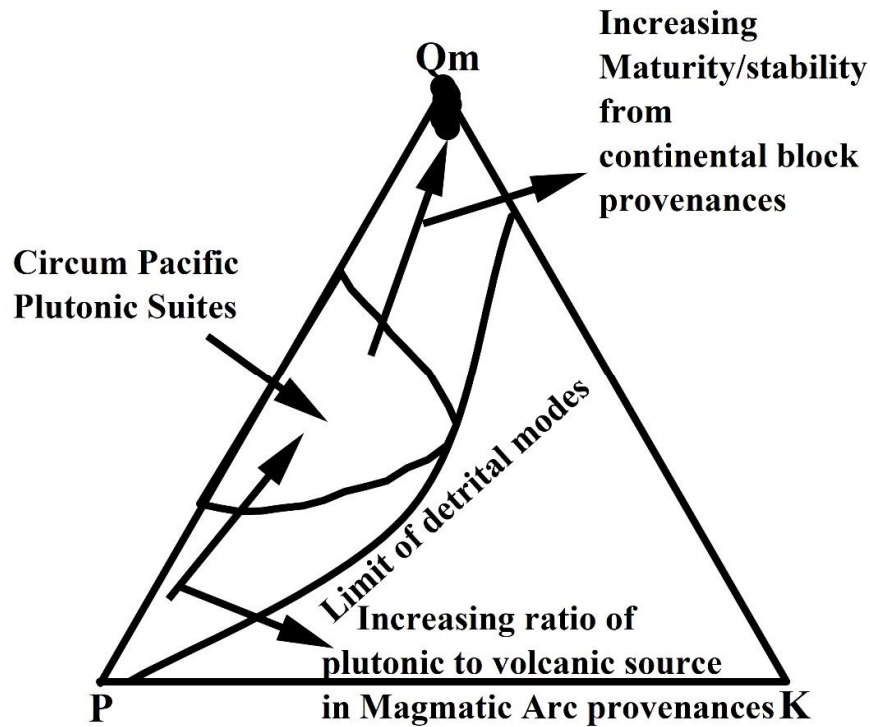


Fig.10.Qm-P-K plot for ox-bow lake sediment of Ganga alluvial plain.

3.5 XRD analysis of ox-bow lake sediments of Ganga alluvial plain

Ten samples were analyzed by XRD (Shimadzu LabX 6100 diffractometer) at the Physics Department of Aligarh Muslim University, from Daryaoganj, Kisaul, Kumraua and Mirpur localities. The XRD analysis reveals that quartz is the major constituent followed by plagioclase in all the samples. The clay minerals are present in variably proportions. Nevertheless, there appears a crude pattern of clay mineral abundance in the samples of different localities as kaolinite-illite-chlorite in descending order (Table.5). Kisaul ox-bow lake sediments possess maximum quartz content (51.70%) but minimum plagioclase (8.33%) and Kaolinite (19.20%) whereas Kumraua ox-bowlake sediments show opposite concentrations of these minerals. Daryaoganj samples are devoid of chlorite mineral (Fig.11).

Table 5. Results of XRD analysis of ox-bow lake (OL) sediments in wt %.

| Location/Minerals | Quartz | Plagioclase | Kaolinite | Illite | Chlorite |
|-------------------|--------|-------------|-----------|--------|----------|
| Daryaoganj (OL) | 47.20 | 13.50 | 26.20 | 13.10 | 0.00 |
| Kumraua (OL) | 40.00 | 10.00 | 30.00 | 15.00 | 5.00 |
| Mirpur (OL) | 46.00 | 12.00 | 24.00 | 12.00 | 6.00 |
| Kisaul (OL) | 51.70 | 8.30 | 19.20 | 15.00 | 5.80 |

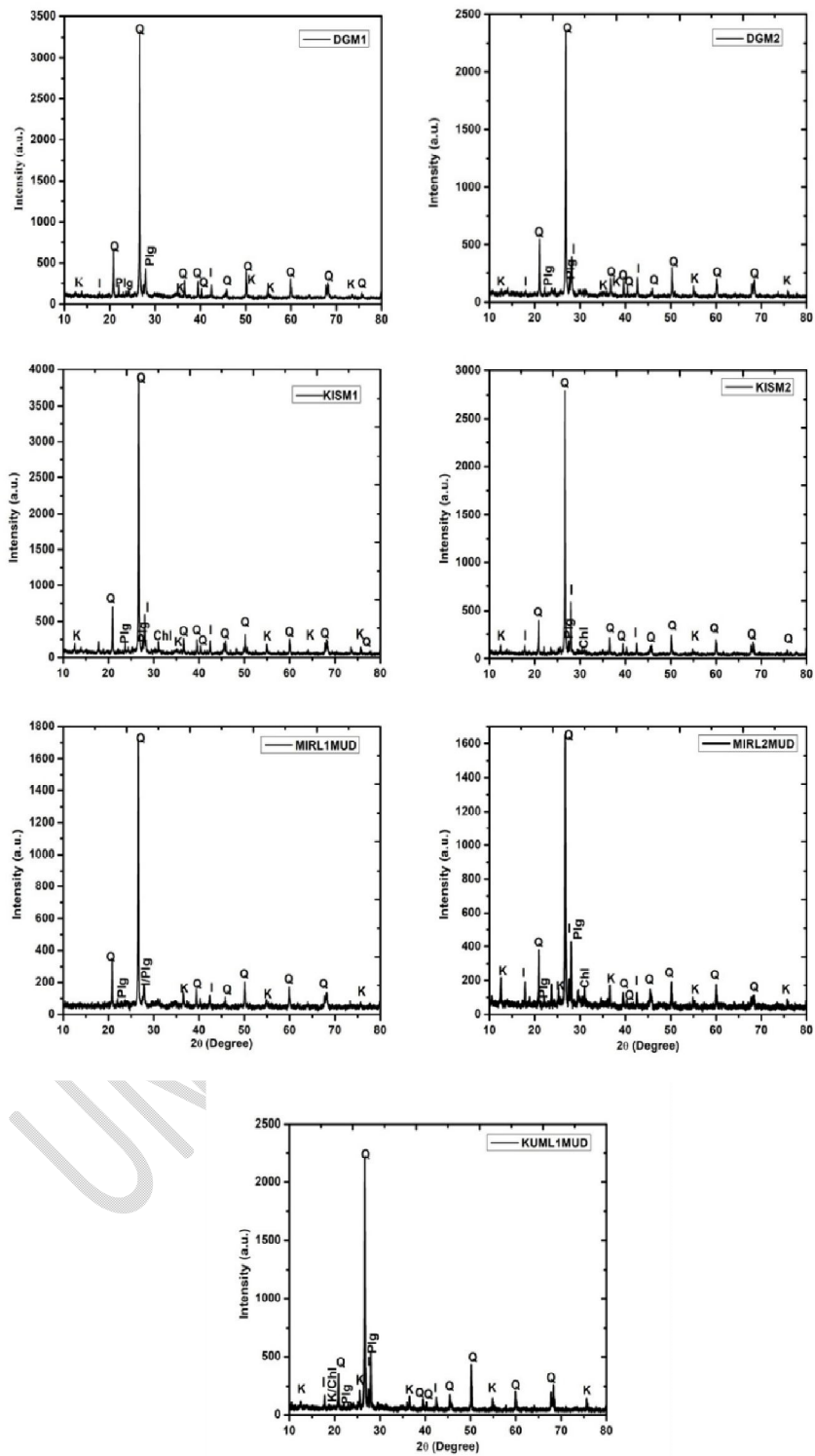


Fig.11. XRD profiles of the finer sediments of ox-bow lake samples.

[79] gave the probable combination of clay minerals originating from different rock types in different tectonic conditions (Table.6). On the basis of the clay mineral contents obtained from XRD (Quartz-Kaolinite-Illite-Chlorite) analysis, the sediments of ox-bow lake appear to have received detritus from craton interior and basement uplift. The clay mineral abundance endorses the interpretation arrived out from Petro-facies plots (Fig.7,8,9&10) for the provenance and tectonic setting of ox-bow lake sediments.

Table 6.Clay mineral assemblages, provenance and tectonic setting after [79].

| Tectonic Setting | Moderate Weathering | Strong weathering |
|--|---|--|
| Igneous Rocks | | |
| Plateau basalts | Fe oxides, smectite, little sand | Fe oxides, some smectite with kaolinite and gibbsite |
| Island arcs | Smectite with volcanoclastic sands | Smectite and kaolinite with volcanoclastic sands |
| Continent-margin arcs | Smectite and illite with quartzofeldspathic and volcanoclastic sands | Smectite, illite and kaolinite with quartz feldspathic and volcanoclastic sands |
| Basement uplifts | Illite with quartzofeldspathic sand | Kaolinite with quartzose sands |
| Sedimentary Rocks | | |
| Fold-thrust belts & strike-slip terranes | Recycled illite, chlorite, kaolinite plus some new smectite; quartzofeldspathic sands | Recycled illite, chlorite, kaolinite plus abundant new kaolinite; quartzose sands |
| Craton interiors | Recycled illite, chlorite and kaolinite; quartzofeldspathic sand | Recycled illite, chlorite and kaolinite plus abundant new kaolinite; quartzose sands |
| Metamorphic Rocks | | |
| Mountain belts | Recycled chlorite, muscovite, illite; quartzofeldspathic sands | Recycled chlorite, muscovite, illite with new kaolinite; quartzose sands |
| Precambrian shields | Recycled muscovite, illite; quartzofeldspathic sands | Recycled muscovite, illite with new kaolinite; quartzose sands |

4. CONCLUSION

With the current effort, we now have a better understanding of the petrography, Petro facies, paleoclimate, provenance and tectonic setting of the sediments of ox-bow lake of Ganga plain. The main conclusions that have been established are as follows: In this study, the detrital minerals found in sediments from ox-bow lake were analyzed to determine their origin. To interpret the provenance of these minerals, triangular diagrams proposed by [10], namely Qt-F-L, Qm-F-Lt, Qp-Lv-Ls, and Qm-P-K, were employed. Both the Qt-F-L and Qm-F-Lt plots depict complete grain populations, but with distinct emphases. The Qp-Lv-Ls and Qm-P-K plots, on the other hand, exhibit partial grain populations while revealing the characteristics of polycrystalline and monocrystalline components of the framework, respectively. The Qt-F-L diagram, which places emphasis on factors influenced by

provenance, relief, weathering, and transport mechanisms, is constructed based on the overall content of quartzose, feldspar, and lithic components. According to [24] the ox-bow lake sediments are mainly fall in sublitharenites field. The dominant constituents of the framework grains are primarily quartz, followed by rock fragments, feldspar, mica, and heavy minerals. The majority of the quartz grains are monocrystalline, while the remaining are polycrystalline. Monocrystalline quartz commonly exhibits undulatory extinctions, whereas polycrystalline quartz grains display both distinct and suture intercrystallite boundaries. The feldspar category comprises both fresh and altered varieties, including plagioclase and microcline. Additionally, the presence of biotite, as well as large flakes of muscovite and mica, has been observed. Within the rock fragments, various types such as quartzite, schist, gneiss, phyllite, chert, sandstone, limestone, and siltstone can be found. The plot of the recalculated values indicates that the majority of the sediments sample from the ox-bow lake fall within the recycled orogen provenance field. This suggests that these sediments are derived from metasedimentary and sedimentary rocks that were initially deposited along former passive continental margins. In the Qm-F-Lt diagram, all unstable lithic fragments, including the polycrystalline quartz, are combined and plotted as Lt to highlight the source rocks. In this diagram, the sample data can be observed to plot within both the recycled orogen and craton interior fields. The Qp-Lv-Ls triangular plot, which is focused on the population of rock fragments, provides insight into the polymineralic components of the source region and offers a more detailed understanding of tectonic elements. It allows for a clearer and more refined depiction of the tectonic characteristics and composition of the source materials. The analyzed data indicates that it falls within the settings of a collisional suture and fold thrust belt source suggesting that there is no contribution from a volcanic source. The Qm-P-K plot reveals that all the sediment contributions in the data originate from the uplifted continental block basement, indicating a provenance characterized by mineralogical maturity and the stability of the source area. The ox-bow lake petrofacies indicate their derivation from cratonic interiors, as well as recycled orogenic and quartzose recycled provenances, under semi-humid to humid climatic conditions. The clay mineral abundance endorses the interpretation arrived out from petrofacies plots for the provenance and tectonic setting of ox-bow lake sediments. The heavy minerals encompass a range of minerals such as tourmaline, garnet, opaques, zircon, kyanite, andalusite, sillimanite, staurolite, epidote, actinolite/tremolite, hornblende, biotite, rutile, muscovite, chlorite, apatite, corundum and zoisite. The presence of various heavy mineral species in the ox-bow lake sediments of the Ganga plain suggests that these sediments originated from a diverse array of source rocks. Tourmaline emerges as the dominant heavy mineral, exhibiting various colors. Brown and blue tourmaline varieties likely originated in pegmatites, while the green variety has roots in granitic rocks [3]. Moreover, rounded tourmaline seems to have been derived from a pre-existing sedimentary source, indicating multiple transportation cycles. The presence of kyanite-sillimanite in these sediments suggests the weathering contribution of kyanite-sillimanite-bearing high-grade metamorphic rocks in the source terrain. Colorless garnet may have originated from schists, light pink garnet from acid igneous rocks like granite, and brownish garnet from igneous metamorphic rocks such as crystalline gneisses and schists. Zircon likely came from crystalline igneous and metaigneous rocks, and apatite from acid igneous rocks and pegmatites. In the contact aureoles around igneous intrusions in meta-argillaceous rocks, andalusite crystallizes. Gneisses and pegmatite granite are the main places where topaz forms. Corundum is present in a variety of rock types, but is most common in Al-rich, Si-poor rocks like mica, chlorite schists, syenites, and quartz free pegmatites.

The preceding discussion on heavy minerals suggests that the sediments in ox-bow lake originated from a diverse mixture of acid and basic igneous rocks and low to high-grade metamorphic rocks. The well-rounded shape of tourmaline indicates its origin from a sedimentary source. The Ganga River, the transporting agent of these sediments, flows through regions of the western and central Himalaya composed of granites, gneisses, schists, with a minor component of volcanics and metamorphosed limestone from the Cambrian and Upper Precambrian ages. In addition to Precambrian slates and phyllite, limestone and shales are also widespread in large parts of the region situated north of the Ganga River.

Acknowledgements

The paper is part of Ph. D thesis of G.A. The authors are thankful to Chairperson, Department of Geology, A.M.U Aligarh, for providing research facilities in the department. Financial assistance from University Grant Commission, New Delhi (UGC-MANF) to Gufran Ali is deeply acknowledged.

REFERENCES

1. Dickinson, W.R., 1988. Provenance and sediment dispersal in relation to paleotectonics and paleogeography of sedimentary basins; In: *New Perspectives in Basin Analysis* (Eds.) Kleinspehn K. L. and Paola C. (Berlin: Springer-Verlag); 3–25 pp.
2. Dickinson, W.R., Beard, L.S., Brakenridge, G.R., Erjavec, J.L., Ferguson, R.C., Inman, K.F., Knepp, R.A., Lindberg, F.A and Ryberg, P.T., 1983. Provenance of north American Phanerozoic sandstones in relation to tectonic setting. *Geological Society of American Bulletin*; v 94; pp 222- 235.
3. Krynine, P.D, 1942. Differential sedimentation and its products during one complete geosynclinal cycle, in primer congress panamericano De Ingeniera de Minas Geology Medidlingen; 20: 142-147.
4. Potter, P. E. (1994). Modern sands of South America: composition, provenance and global significance. *Geologische Rundschau*, 83, 212-232.
5. Garzanti, E., & Andò, S. (2019). Heavy minerals for junior woodchucks. *Minerals*, 9(3), 148.
6. Mange, M. A., & Wright, D. T. (2007). High-resolution heavy mineral analysis (HRHMA): a brief summary. *Developments in Sedimentology*, 58, 433-436.
7. Morton, A.C, 1985. Heavy minerals in provenance studies. In: Zuffa, G.G. (Ed.) *Provenance of Arenites*, D. Reidel, Dordrecht; pp 249-277.
8. Dickinson, W.R and Suczek, C.A., 1979. Plate-tectonics and sandstones composition. *The American Association of Petroleum Geologists Bulletin*; v 63; pp 2164- 2182.
9. Valloni, R and Mezzardi, G., 1984. Compositional suites of terrigenous deep-sea sands of the present continental margins. *Sedimentology*; v 31; pp 353-364.

10. Dickinson, W.R., 1985. Interpreting relations from detrital modes of sandstone. In: G.G. Zuffa (Eds.), *Provenance of Arenites*. Reidel, Dordrecht-Boston-Lancaster; 333-361 pp.
11. Valloni, R., 1985. Reading provenance from modern marine sands. In: G.G. Zuffa (Ed), *Provenance of Arenites*. Reidel, Dordrecht; v 148; pp 309-332.
12. Lucchi, F. R. (1985). Influence of transport processes and basin geometry on sand composition. In *Provenance of Arenites* (pp. 19-45). Dordrecht: Springer Netherlands.
13. Velbel, M. A. (1985). Geochemical mass balances and weathering rates in forested watersheds of the southern Blue Ridge. *American Journal of Science*, 285(10), 904-930.
14. Suttner, L.J., 1974. Sedimentary petrographic provinces: An evaluation. *SEPM Special Publication*; v 21; pp 75-84.
15. Mack, G. H. (1984). Exceptions to the relationship between plate tectonics and sandstone composition. *Journal of Sedimentary Research*, 54(1), 212-220.
16. Basu, A. (1985). Influence of climate and relief on compositions of sands released at source areas. *Provenance of arenites*, 1-18.
17. Suttner, L.J. and Dutta, P.K., 1986. Alluvial sandstones composition and paleoclimate, I, framework mineralogy. *Journal of Sedimentary Petrology*; v 56; pp 329-345.
18. Grantham, J.H and Velbel, M.A, 1988. The influence of climate and topography on rock-fragments abundance in modern fluvial sands of the southern Blue Ridge Mountains, North Carolina. *Jour. Sed. Petrology*; 58:219-227.
19. Girty, G.H, 1991. A note on the composition of plutoniclastic sand produced in different climatic belts, (short notes). *Jour. Sed. Petrology*; 61: 428 - 433.
20. Akhtar, K and Ahmad, A.H.M, 1991. Single-cycle cratonic quartzarenites produced by tropical weathering: the Nimar Sandstone (Lower Cretaceous), Narmada basin, India. *Sed. Geology*; 71: 23-32.
21. Mackei, W, 1896. The sands and sandstones of eastern Moray, Edinburgh. *Geol. Soc. Trans*; 7:148-172.
22. Krynine, P.D, 1940. Petrology and genesis of the Third Bradford sand, *Bull. Pennsylvania Stat Coll. Min. Ind. Expt. Sta*; 29:134P.
23. Krynine, P.D, 1946. Microscopic morphology of quartz types. *An. 2^o Cong. Panames. Ing. Minas. Geology*; 3: 35-49.
24. Folk, R.L, 1980. *Petrology of Sedimentary Rocks*. Hemphills, Austen. Texas; 182P.
25. Blatt, H and Christie, J.M, 1963. Undulatory extinction in quartz of igneous and metamorphic rocks and its significance in provenance studies of sedimentary rocks. *Jour. Sed. Petrology*; 38: 1326 -1339.

26. Fuji, K, 1958. Petrography of the Cretaceous sandstones of Hokkaido, Japan. Kyushu Univ. Fac. Sci. Mem. Ser.D; 6:129-152.
27. Pettijohn, F. J., Potter, P. E., Siever, R., Pettijohn, F. J., Potter, P. E., & Siever, R. (1987). Petrography of common sands and sandstones. Sand and Sandstone, 139-213.
28. Martens, J. H. (1931). Persistence of feldspar in beach sand. American Mineralogist: Journal of Earth and Planetary Materials, 16(11), 526-531.
29. Russell, R. D. (1939). Effects of transportation on sedimentary particles: Part 1. Transportation.
30. Krynine, P. D. (1948). The megascopic study and field classification of sedimentary rocks. The Journal of Geology, 56(2), 130-165.
31. Hayes, J. R. (1962). Quartz and feldspar content in South Platte, Platte, and Missouri River sands. Journal of Sedimentary Research, 32(4), 793-800.
32. Pittman, E.D, 1963. Use of zoned plagioclase as an indicator of Provenance. Jour. Sed. Petrology; 33: 380-386.
33. Rim Saite, J, 1967. Optical heterogeneity of feldspars observed in diverse Canadian rocks. Schweiz. Mem. Pet. Mitt; 47:61-76.
34. Field, M. E and Pilkey, O.H, 1969. Feldspar in Atlantic continental margin sands off the SE United states. Bull. Geol. Soc. America; 80: 2097-2102.
35. Pettijohn, F.J, 1975. Sedimentary Rocks, Harper and Brothers, New York; 628p.
36. Pettijohn, F.J, 1957. Sedimentary Rocks (2nd ed.), New York, Harper and Bros; 718P.
37. Milner, H, B, 1962. Sedimentary Petrography PartII. George Allen and Unwin Ltd.London;715P.
38. Boswell, P.G.H, 1933. Mineralogy of sedimentary rocks. London Thos. Murby and Co; 393 p.
39. Krumbein, W.C and Pettijohn, F.J, 1938. Manual of Sedimentary Petrography. Applaton Century, Inc. New York; 549 p.
40. Feo-Codecido, G, 1956. Heavy mineral techniques and their apphcation to Venezuela stratigraphy. Am. Assoc. Petrol. Geol. BuUettin; 40:984-1000.
41. Ijima, A, 1959. On relationship between the provenance and the depositional basins, considered from the heavy mineral associations of the Upper Cretaceous and Tertiary Formations in central and southeastern Hokkaido, Japan: Jour. Fac. Sci. Univ. Tokyo, sec II; 11 (4): 339-385.
42. Okada, H, 1967. Composition and cementation of some lower Paleozoic grits in Wales. Kyushu Univ. Mem. Fac. Sci.Ser.D, Geology; 18:261-276. Sedimentology; 7:211-232.

43. McCarley, A. B., 1981. Metamorphic terrance favoured over Rocky Mountains as source of Claiborne group, Eocene, Texas Coastal plain, *Jour. Sed. Petrology*; 51: 1267-1276.
44. Singh, LB and Ghosh, D.K, 1994. Geomorphology and neotectonic features of IndoGangetic plain. In:K.R.Dikshit, V.S.Kala and M.N. Kaul (Eds.), *India: Geomorphological Diversity*. Rawat Publicatios, Jaipur; 270 – 286
45. Singh I B 2004 Late Quaternary history of the Ganga Plain; *J. Geol. Soc. India* 64 431–454
46. Sharma, C., Chauhan, M.S., Sharma, M., Sharma, S., Singh, I.B., 2001. Proxy records of Holocene vegetation and climate changes from Sanai Tal, central Ganga Plain. In: *Proceedings of National Symposium on Role of Earth Science and Integrated Development and Related Societal Issue*. Geological Survey of India, Special Publication, vol. 65(3), pp. 199-202.
47. Srivastava, P., Singh, I. B., Sharma, M., & Singhvi, A. K. (2003). Luminescence chronometry and Late Quaternary geomorphic history of the Ganga Plain, India. *Palaeogeography, Palaeoclimatology, Palaeoecology*, 197(1-2), 15-41.
48. Singh, I. B., & Rastogi, S. P. (1973). Tectonic framework of Gangetic alluvium, with special reference to Ganga River in Uttar Pradesh. *Current Science*, 305-307.
49. Derry, L. A., & France-Lanord, C. (1996). Neogene Himalayan weathering history and river $^{87}\text{Sr}/^{86}\text{Sr}$: impact on the marine Sr record. *Earth and Planetary Science Letters*, 142(1-2), 59-74.
50. Dickinson, W. R. (1974). *Tectonics and sedimentation*. SEPM Society for Sedimentary Geology.
51. Sieber, L., Arbuster, J. G and Quittmeyer, R. C, 1981. Seismicity and continental Subduction in the Himalayan arc, p. 215- 242. In: *Zagros, Hindukush, Himalaya Geodynamic evolution*, (Eds. Gupta, H. K. and Delany, F. M.), Am. Geophys. U., Washington, Geodynamic Series 3.
52. Molnar, P., & Tapponnier, P. (1975). Cenozoic Tectonics of Asia: Effects of a Continental Collision: Features of recent continental tectonics in Asia can be interpreted as results of the India-Eurasia collision. *science*, 189(4201), 419-426.
53. Ni, J., & Barazangi, M. (1984). Seismotectonics of the Himalayan collision zone: Geometry of the underthrusting Indian plate beneath the Himalaya. *Journal of Geophysical Research: Solid Earth*, 89(B2), 1147-1163.
54. Molnar, P, 1984, Structures and tectoncs of the Himalaya: constrains and implications of geophysical data. *Am. Rev. Earth Planet. Science*; 12: 489- 518.
55. Singh, I.B, 1996. Late quaternary sedimentation of Ganga plain foreland basin, preoc. symp. NW Himalaya and foredeep, feb. 1995. *Geol. Surv. India, Spl.pub*; 21(2): 161-172.

56. Burbank, D. W., Beck, R. A., Mulder, T., Yin, A., & Harrison, T. M. (1996). The Himalayan foreland basin. *World and regional geology*, 149-190.
57. DeCelles, P. G., Gehrels, G. E., Quade, J., & Ojha, T. P. (1998). Eocene-early Miocene foreland basin development and the history of Himalayan thrusting, western and central Nepal. *Tectonics*, 17(5), 741-765.
58. France - Lanord, C, Derry, L and Michard, A, 1983. Evolution of Himalaya since Miocene time: isotopic & Sedimentological evidence from the Bengal fan. In: Trelor, P.J. & Searl, M.P. (eds.) *Himalayan Tectonics*. Geological society, special publication, 74: 603-621.
59. Covey, M. (1986). The evolution of foreland basins to steady state: evidence from the western Taiwan foreland basin. *Foreland basins*, 77-90.
60. Burbank D. W, 1992. Causes of recent Himalayan uplift deduced from deposited patterns in the Ganga basin, *Nature*; 357: 680-683.
61. Valdiya, K. S. (1980). The two intracrustal boundary thrusts of the Himalaya. *Tectonophysics*, 66(4), 323-348.
62. Krynine, P.D, 1940. Petrology and genesis of the Third Bradford sand, *Bull. Pennsylvania Stat Coll. Min. Ind. Expt. Sta*; 29:134P.
63. Fuchtbauer, H, 1974. *Sediments and sedimentary rocks: Part H*, John Wiley & sons, New York, 464p.
64. Rittenhouse, C, 1943. Transportation and deposition of heavy minerals. *Bull. Geol. Soc. America*; 45: 1725- 1780.
65. Milner, H, B, 1962. *Sedimentary Petrography Part II*. George Allen and Unwin Ltd. London; 715P.
66. Cox, R., & Lowe, D. R. (1996). Quantification of the effects of secondary matrix on the analysis of sandstone composition, and a petrographic-chemical technique for retrieving original framework grain modes of altered sandstones. *Journal of Sedimentary Research*, 66(3), 548-558.
67. Triebold, S., von Eynatten, H., Luvizotto, G. L., & Zack, T. (2007). Deducing source rock lithology from detrital rutile geochemistry: an example from the Erzgebirge, Germany. *Chemical geology*, 244(3-4), 421-436.
68. Meinhold, G. (2010). Rutile and its applications in earth sciences. *Earth-Science Reviews*, 102(1-2), 1-28.
69. Triebold, S., von Eynatten, H., & Zack, T. (2012). A recipe for the use of rutile in sedimentary provenance analysis. *Sedimentary Geology*, 282, 268-275.
70. Morton, A.C., 1987. Influences of provenance and diagenesis on detrital garnet suites in the Forties sandstone, Paleocene, central North Sea. *Journal of Sedimentary Petrology* 57, 1027-1032.

71. Mange, M. A., & Morton, A. C. (2007). Geochemistry of heavy minerals. *Developments in sedimentology*, 58, 345-391.
72. Krippner, A., Meinhold, G., Morton, A. C., & von Eynatten, H. (2014). Evaluation of garnet discrimination diagrams using geochemical data of garnets derived from various host rocks. *Sedimentary Geology*, 306, 36-52.
73. Stutenbecker, L., Berger, A., & Schlunegger, F. (2017). The potential of detrital garnet as a provenance proxy in the Central Swiss Alps. *Sedimentary geology*, 351, 11-20.
74. Blatt, H., Middleton, G. V., And Murray, R. C., 1980, *Origin of Sedimentary Rocks* (2nd ed.): Englewood Cliffs, NJ, Prentice-Hall, 782 p.
75. Friedman, G. M and Johnson, K. G, 1982. *Excise in sedimentology*, John wiley & Sons, New York, 65- 99.
76. Weltje, G. J., Meijer, X. D., & De Boer, P. L. (1998). Stratigraphic inversion of siliciclastic basin fills: a note on the distinction between supply signals resulting from tectonic and climatic forcing. *Basin research*, 10(1), 129-153.
77. Graham, S. A., Ingersoll, R. V., & Dickinson, W. R. (1976). Common provenance for lithic grains in Carboniferous sandstones from Ouachita Mountains and Black Warrior Basin. *Journal of Sedimentary Research*, 46(3), 620-632.
78. Ingersoll, R.V and Suczek, C.A, 1979. Petrology and provenance of Neogene sand from Nicobar and Bengal Fans, DSDP sites 211 and 218. *Jour. Sed. Petrology*; 49:1217-1218.
79. Potter, P.E., 2005. Provenance of Mudstones. *Mud and Mudstones*; 157-174 pp.